Supplementary Methods

Bisulphite sequencing analyses. Nested or semi-nested PCR was conducted on converted DNA using primers specific for each of the elements analyzed (primer sequences are listed in Supplementary Information, Table 1). Amplification products were cloned via T/A cloning using the pGEM-T easy kit (Promega) and individual clones were sequenced using BigDye v3.1 chemistry. Sequences were analyzed using Sequencher software (Gene Codes). The mean number of methylated CpGs (mCpGs)/molecule sequenced is presented for each set of samples. As the number of CpGs in the 5'LTR regions of ERVs is heterogeneous, a CpG density "key" is not shown for these elements.

Northern and Southern analysis. Genomic DNA was extracted using DNAzol (Invitrogen) according to the manufacturer's instructions. For each digested sample, 2-3 mg of genomic DNA was loaded per lane. LTR-specific probes were used for analysis of IAP and MLV elements. Probes were labeled with [α-^{32}P]dCTP using the Random Primers DNA Labeling System (Invitrogen). Membranes were pre-hybridized in ExpressHyb (BD Biosciences) at 60°C for 3-5 hours, hybridized overnight at the same temperature in fresh ExpressHyb, washed according to the manufacturer's protocol and exposed to film.

For Northern analyses, total RNA was extracted using the RNeasy RNA isolation kit (Qiagen) according to the manufacturer's instructions. For each lane, 5-8 mg of RNA was denatured, subject to electrophoresis in a 0.8% agarose, 1.9% formaldehyde gel in

1xMOPS buffer and transferred overnight to a Zeta-probe nylon membrane (Bio-Rad). MusD, IAP and MLV specific probes were labeled with [α-^{32}P]dCTP as above. Membranes were pre-hybridized at 68°C for 3-5 hours, hybridized overnight at the same temperature in fresh ExpressHyb, washed according to the manufacturer's protocol and exposed to film. The probes for the MusD *gag* region and the IAP *pol* gene were synthesized by PCR from C57BL6 genomic DNA.

ChIP experiments. ChIP for histones was conducted as described (Appanah et al, 2007). Briefly, 2.4-4x10^7 exponentially growing ES cells were incubated in the presence of 1% (v/v) formaldehyde for 10 minutes at 37°C and chromatin was sonicated to fragment sizes of 300-1000bp using the Bioruptor sonicator (Diagenode). Purified, reverse-crosslinked material was resuspended in 50 ml elution buffer (Qiagen) and quantified by real-time quantitative PCR using 2 µl of template with EvaGreen dye and hot-start Taq polymerase (Fermentas). ChIP for non-histone proteins was conducted as described (O'Geen et al, 2007). Purified rabbit IgG (10µg, Sigma) was used as a control. Antibodies specific for H3 (2.5µg; Abcam, ab1791), H3K9me2 (5µg; Upstate, 07-441), H3K9me3 (5µg; Upstate, 07-442 or 2.5-5µg; Abcam, ab8898), HP-1α (kind gift of Stephen Smale), and Dnmt3a (5µg; Imgenex, IMG-268A) were used. Of note, while Dnmt3a2 is the predominant protein recognized by the Dnmt3a "specific" antibody, this reagent also shows weak cross-reactivity with Dnmt3b1, as determined by Western blotting (Chen et al, 2002).

Reactions were carried out in triplicate (conditions available upon request). For each amplicon, the amount of input and immunoprecipitated DNA was calculated using the standard curve method. The "percent of input" was subsequently calculated by taking the ratio of these values. For the major satellite amplicon, DNA was diluted 1:500 prior to PCR.

MeDIP and real-time PCR. Genomic DNA was isolated from 2-3 independent passages of wildtype, G9a$^{-/-}$ and G9a$^{-/-}$Tg ES cells and prepared for MeDIP as previously described (Weber et al, 2007). In brief, 2µg sonicated (300-1000bp) genomic DNA was precipitated with 2µg antibody against 5-methylcytidine (Eurogentec, BI-MECY-1000) and bound DNA was recovered with 8µl M-280 Sheep anti-mouse IgG Dynabeads (Invitrogen). For real-time PCR, 30 ng sonicated genomic input DNA and 1/40 of a MeDIP reaction were used as template and quantified with SYBR Green PCR mastermix (Applied Biosystems) using standard cycling conditions on an ABI Prism 7000 detection system. Relative enrichments were determined by normalizing against an active gene (Hprt). Reactions were performed in duplicates, averaged for each PCR and standard errors were calculated between the averaged duplicate reactions of biological replicate experiments. Primers for DNA methylated loci in ES cells were chosen based on a recent genome-wide study (Mohn et al, 2008) and are listed in Supplementary Table 1.

Western analysis. For Western blotting, 60-100 µg of nuclear extract was added per lane and quantitative western analyses were conducted using the Odyssey Infrared Imaging System (LI-COR Biosciences), according to the manufacturer's protocol. Antibodies

used include: G9a (1:2000; PPMX, A8620A), GLP (1:1000; PPMX, B0422), Suz12 (Kind gift from Yi Zhang), Bmi1 (1:6000; Upstate, 05-637), TFII-I (1:2000; kind gift of Ivan Sadowski), Dnmt1 (1:300; Imgenex, IMG-261A), Dnmt3A (1:300; IMG-268A) and Dnmt3b (1:1000; Imgenex, IMG-184A).

Supplementary References

Appanah R, Dickerson DR, Goyal P, Groudine M, Lorincz MC (2007) An unmethylated 3' promoter-proximal region is required for efficient transcription initiation. *PLoS Genet* **3:** e27

Mohn F, Weber M, Rebhan M, Roloff TC, Richter J, Stadler MB, Bibel M, Schubeler D (2008) Lineage-specific polycomb targets and de novo DNA methylation define restriction and potential of neuronal progenitors. *Mol Cell* **30:** 755-766

O'Geen H, Squazzo SL, Iyengar S, Blahnik K, Rinn JL, Chang HY, Green R, Farnham PJ (2007) Genome-wide analysis of KAP1 binding suggests autoregulation of KRAB-ZNFs. *PLoS Genet* **3:** e89

Tachibana M, Ueda J, Fukuda M, Takeda N, Ohta T, Iwanari H, Sakihama T, Kodama T, Hamakubo T, Shinkai Y (2005) Histone methyltransferases G9a and GLP form heteromeric complexes and are both crucial for methylation of euchromatin at H3-K9. *Genes Dev* **19:** 815-826

Weber M, Hellmann I, Stadler MB, Ramos L, Paabo S, Rebhan M, Schubeler D (2007) Distribution, silencing potential and evolutionary impact of promoter DNA methylation in the human genome. *Nat Genet* **39:** 457-466

Supplementary Figure Legends

Supplementary Figure S1. Western analyses of G9a and GLP expression in the TT2, *G9a*-/-, *G9a*-/-*Tg*, *GLP*-/- and *GLP* -/-*Tg* lines. (A) Nuclear extract was isolated from TT2, *G9a*-/- and *G9a*-/-*Tg* lines and analyzed by Western blotting using antibodies specific for G9a and Suz12 as a loading control. While no G9a expression was detected in the *G9a*-/- line, a significant level of G9a expression was detected in the *G9a*-/-*Tg* line. (B) Similarly, while no expression of GLP was detected in the *GLP*-/- line, a significant level of GLP was detected in the *GLP* -/-*Tg* line. These data confirm that G9a and GLP transgenes are stably expressed in the *G9a*-/-*Tg* and *G9a*-/-*Tg* lines, respectively.

Supplementary Figure S2. MusD ERVs show a dramatic reduction in DNA methylation density in *G9a*-/- cells. Bisulphite analysis of TT2, *G9a*-/-, *Dnmt1*-/- and *G9a*-/-Tg was conducted using primers specific for the 5' LTR and downstream regions of MusD. In the *G9a*-/- and *Dnmt1*-/- lines, these class II ERVs show a significantly lower level of methylation across the LTR and downstream region than in the TT2 line. Introduction of a G9a transgene (*G9a*-/-Tg) rescues the observed DNA methylation defect. The mean number of CpGs/molecule sequenced is shown to the right of each set of sequenced samples, along with the mean % of mCpGs relative to the wildtype line (in parentheses).

Supplementary Figure S3. Major satellite repeats show a DNA methylation defect in G9a-/- ES cells. Genomic DNA isolated from R1 and *Suv39h1/2*$^{-/-}$ lines as well as TT2,

G9a-/-, *G9a-/-* (2-3), *G9a*$^{-/-}$Tg (15-3), J1, *Dnmt1*$^{-/-}$ and *Dnmt3a/b*$^{-/-}$ lines was digested with the methylation-sensitive restriction enzyme HpyCH4IV and subject to Southern analysis using a probe specific for major satellite repeats. The *G9a-/-* line shows a DNA methylation defect similar to that observed in the *Suv39h1/2*$^{-/-}$, *Dnmt1*$^{-/-}$ and *Dnmt3a/b*$^{-/-}$ lines, but not in the parent lines from which these mutants were derived. This defect is reversed in the *G9a*$^{-/-}$Tg line.

Supplementary Figure S4. DNA methylation of MLV and IAP ERVs is reduced in *GLP*$^{-/-}$ cells. (A) Genomic DNA isolated from TT2 *wt*, *GLP*$^{-/-}$ and *GLP*$^{-/-}$Tg lines was digested with HpaII (H) and subject to Southern blotting using probes specific for MLV or IAP elements. While the *GLP*$^{-/-}$ line shows a dramatic reduction in DNA methylation relative to the TT2 parent line, the *GLP* $^{-/-}$Tg line shows a significantly higher level of DNA methylation of both ERVs. (B) Bisulphite analysis confirms that a significantly lower level of methylation is present across the 5' LTR of endogenous MLV elements in the *GLP*$^{-/-}$ line. The mean number of mCpGs/molecule sequenced (combined with the data shown in Figure 1d for the TT2 line) is shown to the right of each set of sequenced samples, along with the mean % of mCpGs relative to the wildtype line (in parentheses).

Supplementary Figure S5. MusD ERVs are transcriptionally silent in *G9a-/-* cells. (A) Northern analysis or RNA isolated from J1, *Dnmt3a/b-/-*, *Dnmt1-/-*, TT2, *G9a-/-* and *G9a-/-*Tg lines reveals aberrant expression of MusD elements (~7.5 kb) in the *Dnmt1-/-* line, but not the *Dnmt3a/b-/-* or *G9a-/-*, or *G9a-/-*Tg lines. Longer exposure of the blot revealed a low level of expression in the *wt* and *G9a-/-* lines (data not shown). (B)

Quantitative RT-PCR (+/-RT) using primers specific for MusD elements revealed a significantly higher level of expression in the *Dnmt1-/-* line than the *G9a-/-* line, consistent with the results obtained by Northern blotting.

Supplementary Figure S6. The promoter region of the Mage-a2 gene is marked by H3K9me2 but not H3K9me3 in wildtype ES cells. ChIP was conducted on *wt* and *G9a-/-* ES cells using antisera specific for H3K9me2, H3K9me3, unmodified H3 and non-specific IgG as a control. Real-time PCR was carried out using primers specific for the promoter region of the Mage-a2 gene. Enrichment (+/-SD) is presented as the percentage of input material immunoprecipitated. A significantly lower level of enrichment of H3K9me2 was detected in the *G9a-/-* line than the *wt* parent line at the promoter region of the Mage-a2 gene. In contrast, both lines showed only very low levels of enrichment of H3K9me3 in this region. The lower level of H3 occupancy observed in the *G9a-/-* line likely reflects transcription-coupled depletion of nucleosomes in the promoter region of the Mage-a2 gene, which is aberrantly expressed in this line (Tachibana et al, 2002).

Supplementary Figure S7. Stable expression of a catalytically inactive G9a transgene in G9a-/- ES cells rescues the DNA methylation defect at MusD elements. Bisulphite analysis of the *G9a-/-* line 2-3 stably transfected with constructs encoding a *wt* G9a transgene *G9a-/-*Tg(*wt*), or the mutant G9a transgenes *G9a-/-*Tg(C1168A) was conducted using primers specific for the 5' LTR and downstream regions of MusD. The mean number of mCpGs/molecule sequenced is shown, along with the mean % of mCpGs relative to the wildtype line (in parentheses). Taken together with the data shown

in figure S2 (bar graph), these data confirm that expression of catalytically inactive G9a rescues the DNA methylation defect observed in the parent *G9a-/-* line. Interestingly, the clone expressing the wildtype transgene, which is expressed at significantly higher levels than the endogenous protein (see Figure 7A) shows a higher level of methylation than the TT2 parent line, suggesting that expression of endogenous G9a is limiting with respect to its influence on DNA methylation in ES cells.

Table 1. Primers used in this study

RT-PCR		
β-actin	+	TCATGAAGTGTGACGTTGACATCCGT
	-	CCTAGAAGCACTTGCGGTGCACGATGGAG
MusD	+	GTGGTATCTCAGGA(G/A)GAGTGCC
		GGGCAGCTCCTCTATCTGAGTG
IAP	+	AAGCAGCAATCACCCACTTTGG
	_	CAATCATTAGATG(T/C)GGCTGCCAAG
Dnmt1	+	TCGGCTGAACAACCCCGGCACCAC
	_	CTTCAGCACCATGGAGCGTCTGTAGG
Dnmt3a	+	GTCCGCAGCGTCACACAGAAGC
	_	TCTTTGGCGTCAATCATCACGG
Dnmt3b	+	AGGTTTATATGAGGGCACAGGAAGGC
	_	CATGTTGGACACGTCCGTGTAGTGAGC
Dnmt3L	+	ACTGAGGATGACCAAGAGACAAC
	_	CTCTTCAGCCCTGGAATGTTGCTC
Bisulfite analysis		Y= C or T, R= A or G
MLV 1st round:	+	TATTTTGTAAGGTATGAAAAAGTATTAGAGT
(RLTR4_Mm-int)	-	AAATCRATAATCCCTAAACAAAAATCTCCA
2nd round:	+	TAAATTTGTGTGTTTGTTAATGTTTTGATT
	-	AAATCRATAATCCCTAAACAAAAATCTCCA
IAP 5'LTR 1st round:	+	GGYGTTGATAGTTGTGTTTTAAGTGGTAAAT
	-	ATTCTAATTCTAAAATAAAAAATCTTCCTTA
2nd round:	+	GATAGTTGTGTTTTAAGTGGTAAATAAATA
	-	ATTCTAATTCTAAAATAAAAAATCTTCCTTA
MusD 5'LTR 1st round:	+	AAATTTGAGTTTTGATTAGTATGAAATTGT
	-	AATCTAATATTTCTTCTTCCTTAAACCATA
2nd round:	+	AAATTTGAGTTTTGATTAGTATGAAATTGT
	-	AACTTTAAACCCTTTCTTCTTCCACCTAAA
Dazl 1st round:	+	GGTTYGAGTTTTATTGATAGATAGATGGAT
	-	AACACCCTACAACTCAACTCTACTATAA
2nd round:	+	GATTTTTGTTATTTTTTAGTTTTTTTAGGAT
	-	AAAATTCTCTCAACTAACCTAACTTATTTCT
Tuba3 1st round:	+	TTAGGGGYGGTTTTAGGTTTTATATTTTAT
	-	ATTACCACCAAACATAACACACATCTATAA
2nd round:	+	ATTTTATTAATGATTGGATGTGGTTTAA
	-	AAATAAACAACTACTCACACAAACTTCC
ChIP analysis		
Major satellite	+	GACGACTTGAAAAATGACGAAATC
	-	CATATTCCAGGTCCTTCAGTGTGC
***IAP* (LTR)**	+	CTCCATGTGCTCTGCCTTCC
	-	CCCCGTCCCTTTTTTAGGAGA
MusD (LTR)	+	CCCTTCCTTCATAACTGGTGTCGCA
	-	TAGCATCTCTCTGCCATTCTTCAGG
Mage-a2	+	TTGGTGGACAGGGAAGCTAGGGGA
	-	CGCTCCAGAACAAAATGGCGCAGA
Primers used for generating Probes		

MusD (gag)	+	GAGTTGTTTCAGGCCAGAGGAGTAAGG
	-	GGGCAGCTCCTCTATCTGAGTG
IAP (LTR) Southern	+	CAGAAGATTCTGGTCTGTGGTGTT
	-	GAATTCATACAGTTGAATCCTTCT
IAP (pol) Northern	+	AAGCAGCAATCACCCACTTTGG
	-	CAATCATTAGATG(T/C)GGCTGCCAAG
MLV (LTR)	+	CATGTGAAAGACCCCACCTGTAG
	-	AGTCGGATGCAACTGCAAGAGGG
Major satellite	+	GACGACTTGAAAAATGACGAAATC
	-	CATATTCCAGGTCCTTCAGTGTGC
LINE1 (L1Md-A2)	+	TCCCAACATAGAGTCCTGAG
	-	TCAGTGGGCAGAGTATTCTC
Primers used for meDIP		
MusD f		CCCTTCCTTCATAACTGGTGTCGCA
MusD r		TAGCATCTCTCTGCCATTCTTCAGG
IAP f		CTCCATGTGCTCTGCCTTCC
IAP r		CCCCGTCCCTTTTTTAGGAGA
Mage f		TTGGTGGACAGGGAAGCTAGGGGA
Mage r		CGCTCCAGAACAAAATGGCGCAGA
Gapdh f		CTCTGCTCCTCCCTGTTCC
Gapdh r		TCCCTAGACCCGTACAGTGC
Sycp1 f		TGGACCAACCGTTAAATTGAG
Sycp1 r		GCGCTCCTTTATGAAGACGA
Brdt f		GCGGGTGAGTCCCATAAAG
Brdt r		CGATCACCCTTTCAGTTTGC
Interg3 f		ATGCCCCTCAGCTATCACAC
Interg3 r		GGACAGACATCTGCCAAGGT
Rho f		CTGGAGCCATGTGGAGAAGT
Rho r		GGTGGAGGCCCTTAGGTAAA
Il12a f		CAGTGTCCACGATGGAGAGA
Il12a r		ACCACACTCAGAGCGAAAGC
Lrrtm2 f		CTTCCCGCAGCTGTTAGTTC
Lrrtm2 r		TCGCAGCACATAAGCAAATC
H19_ICR f		GCATGGTCCTCAAATTCTGCA
H19_ICR r		GCATCTGAACGCCCCAATTA
Hprt f		AGCGTTTCTGAGCCATTGCT
Hprt r		GCAAAAAGCGGTCTGAGGAG
Dazl f		AATGCCCGCAGAAATAGAAA
Dazl r		TTCGGGCATTTATTTGAAGG
Spo11 f		CCAAACCAGGCAGAAATGTT
Spo11 r		ATCTCTGGGGTCGAGGTTTT
Gtl_ICR f		CTTTTGTTGACCACAACCCTTG
Gtl_ICR r		AATCCCACCACAGCTTCTTAGC
Tuba3 f		GCGCAGATAACATACGCAGA
Tuba3 r		ATGTGGCTCAAGTTGCAGTG

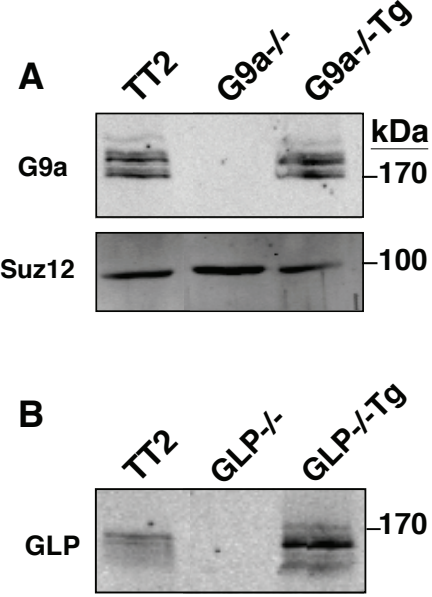

Figure S1

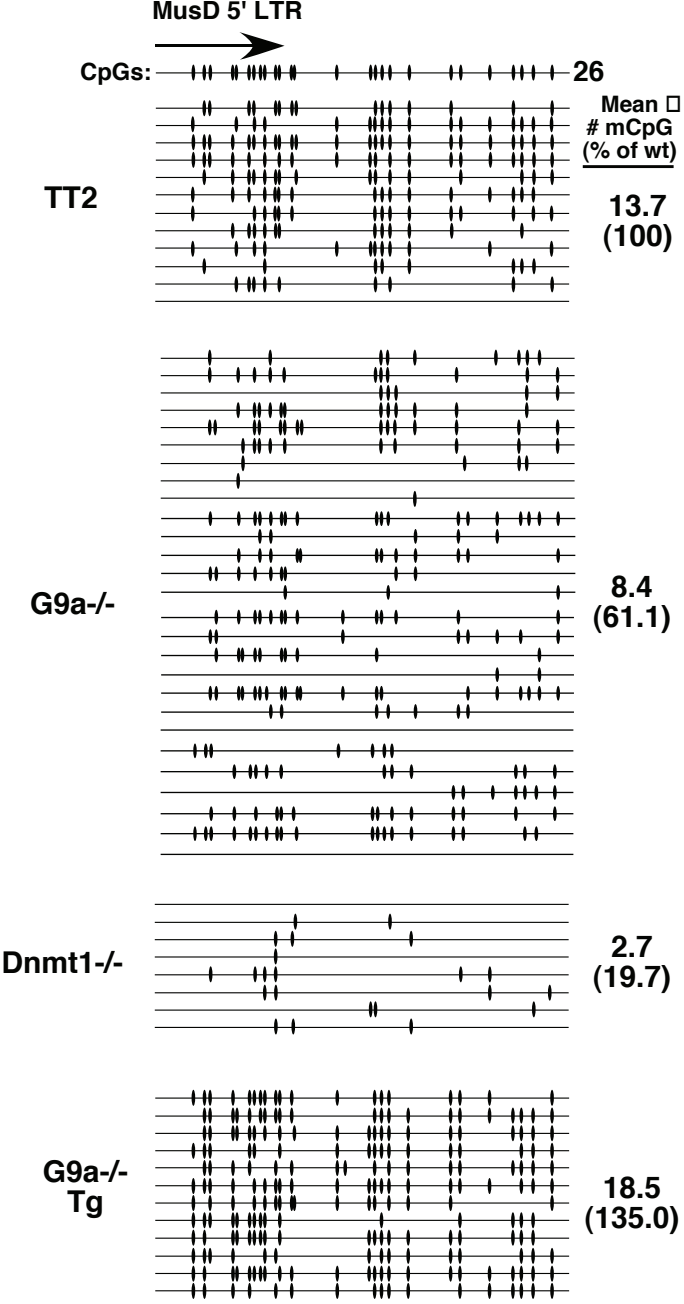
MusD 5' LTR
CpGs:
26
Mean # mCpG (% of wt)
TT2
13.7
(100)
G9a-/-
8.4
(61.1)
Dnmt1-/-
2.7
(19.7)
G9a-/-
Tg
18.5
(135.0)

Figure S2

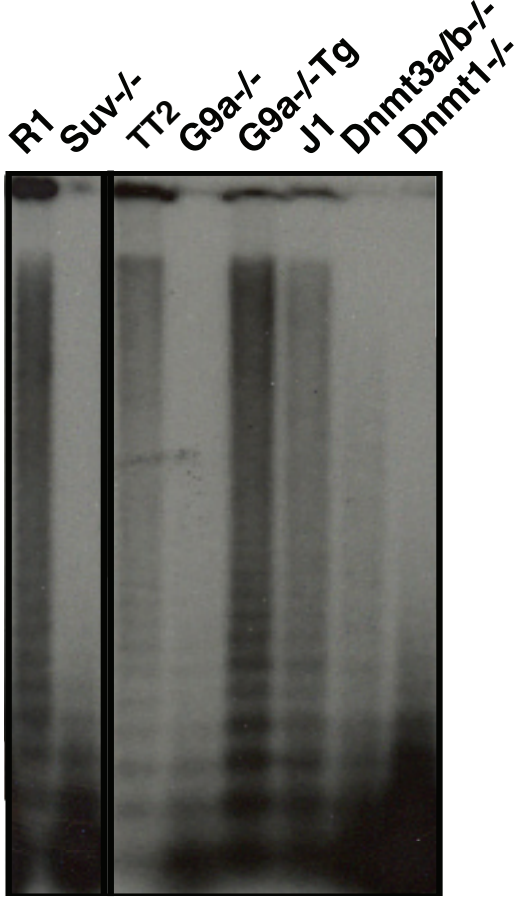

Major Satellite

Figure S3

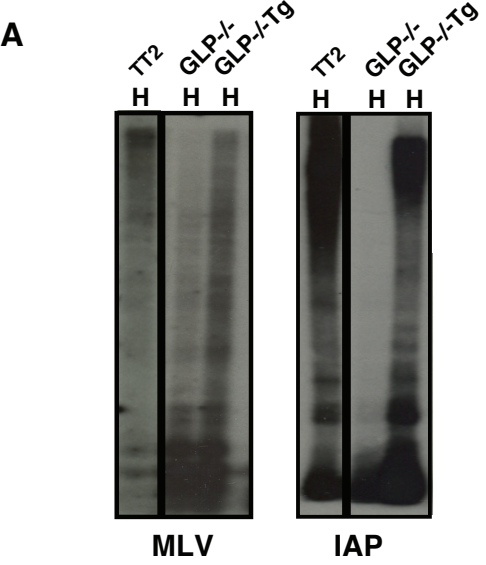
A
TT2
GLP-/-
GLP-/-Tg
H H H
TT2
GLP-/-
GLP-/-Tg
H H H
MLV
IAP

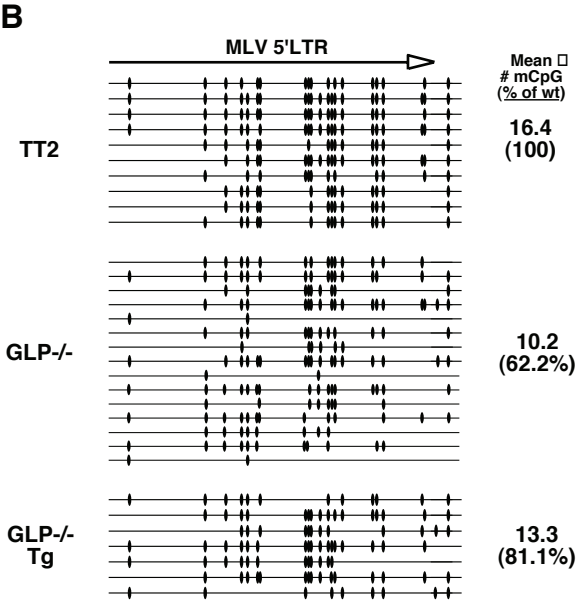
B
MLV 5'LTR
Mean # mCpG (% of wt)
TT2
16.4 (100)
GLP-/-
10.2 (62.2%)
GLP-/- Tg
13.3 (81.1%)

Figure S4

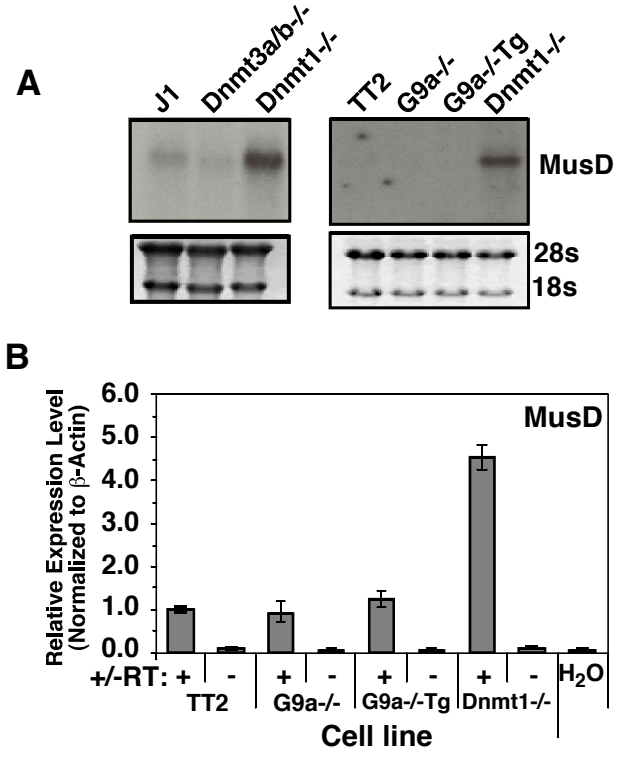
A
J1
Dnmt3a/b-/-
Dnmt1-/-
TT2
G9a-/-
G9a-/-Tg
Dnmt1-/-
MusD
28s
18s
B
Relative Expression Level
(Normalized to β-Actin)
6.0
5.0
4.0
3.0
2.0
1.0
0.0
MusD
+/-RT: + - + - + - + - H2O
TT2
G9a-/-
G9a-/-Tg
Dnmt1-/-
Cell line

Figure S5

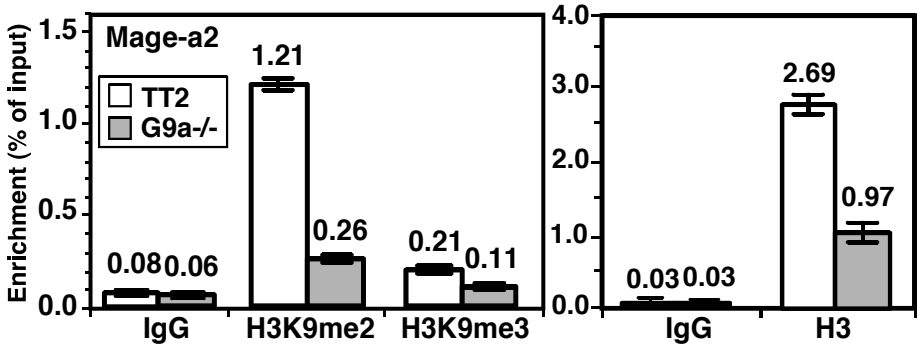
Mage-a2
TT2
G9a-/-
Enrichment (% of input)
1.5
1.0
0.5
0.0
0.08
0.06
1.21
0.26
0.21
0.11
IgG
H3K9me2
H3K9me3
4.0
3.0
2.0
1.0
0.0
0.03
0.03
2.69
0.97
IgG
H3

Figure S6

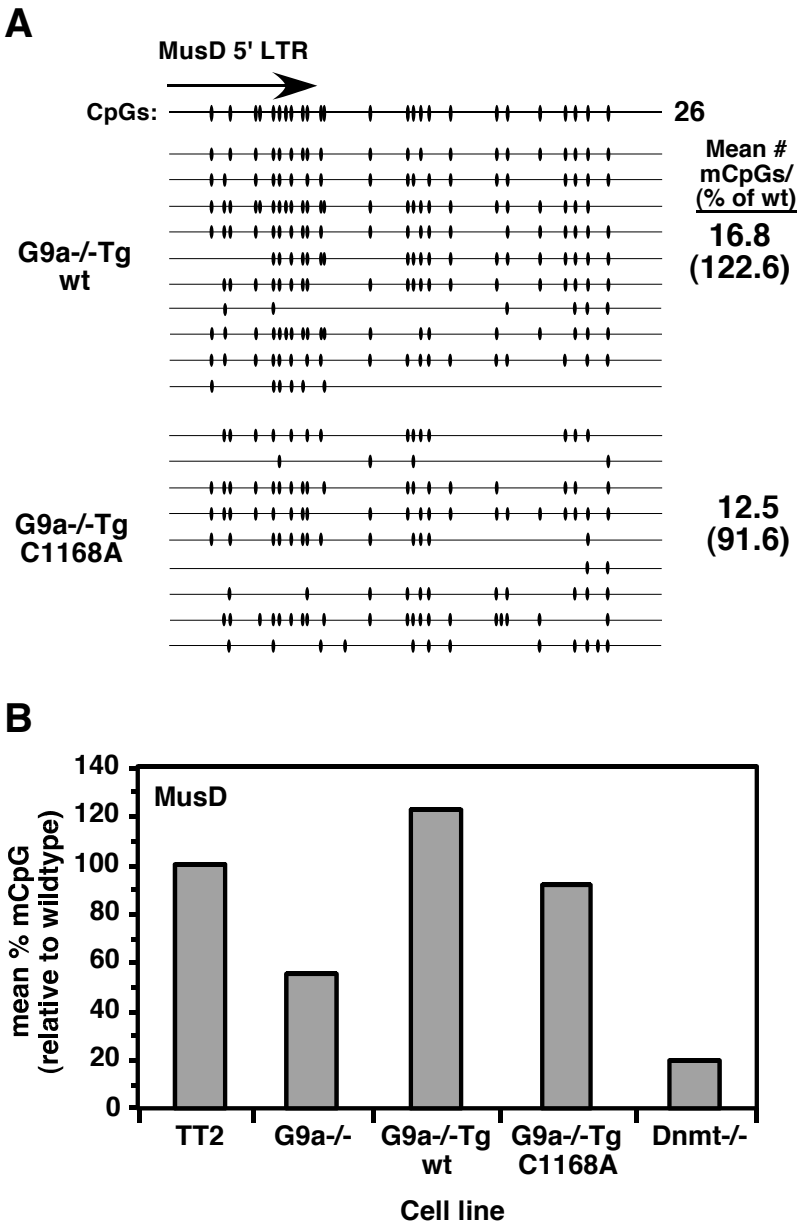
A
MusD 5' LTR
CpGs:
26
Mean # mCpGs/ (% of wt)
G9a-/-Tg wt
16.8 (122.6)
G9a-/-Tg C1168A
12.5 (91.6)
B
MusD
mean % mCpG (relative to wildtype)
140
120
100
80
60
40
20
0
TT2
G9a-/-
G9a-/-Tg wt
G9a-/-Tg C1168A
Dnmt-/-
Cell line

Figure S7